Article

London University Search Instrument: A Combinatorial Robot for High-Throughput Methods in Ceramic Science

Jian Wang, and Julian R. G. Evans

J. Comb. Chem., **2005**, 7 (5), 665-672• DOI: 10.1021/cc050006q • Publication Date (Web): 06 August 2005

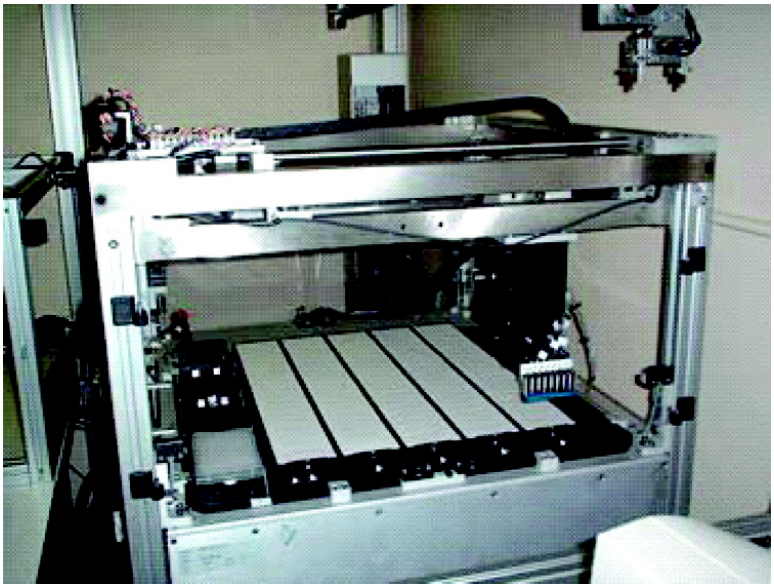

London University Search Instrument: A Combinatorial Robot for High-Throughput Methods in Ceramic Science

Jian Wang and Julian R. G. Evans*

Department of Materials, Queen Mary, University of London, Mile End Road, London, E1 4NS, United Kingdom

Received January 11, 2005

This paper describes the design, construction, and operation of the London University Search Instrument (LUSI) which was recently commissioned to create and test combinatorial libraries of ceramic compositions. The instrument uses commercially available powders, milled as necessary to create thick-film libraries by ink-jet printing. Multicomponent mixtures are prepared by well plate reformatting of ceramic inks. The library tiles are robotically loaded into a flatbed furnace and, when fired, transferred to a 2-axis high-resolution measurement table fitted with a hot plate where measurements of, for example, optical or electrical properties can be made. Data are transferred to a dedicated high-performance computer. The possibilities for remote interrogation and search steering are discussed.

Introduction

High-throughput techniques and informatics have brought about major methodological changes in medicinal and synthetic chemistries which are now beginning to impact on the materials sciences in metallurgy,[1] polymer synthesis,[2] and ceramics.[3] It is appropriate that Joseph Hanak, often credited with helping to usher in the age of high-throughput screening published his often-cited "chronic ailment" quotation in *Journal of Materials Science* in 1970:[4] "The present approach to the search for new materials suffers from a chronic ailment, that of handling one sample at a time in the processes of synthesis, chemical analysis and testing of properties. It is an expensive and time-consuming approach, which prevents highly trained personnel from taking full advantage of its talents and keeps the tempo of discovery of new materials at a low level."

One of the earlier attempts to perform automated combinatorial searches for new ceramics was conducted at the GEC Hirst Research Centre in the late 1980s in a quest for new ceramic superconductor compositions. In this pioneering approach, a robot was used to mix up to nine aqueous chelated solutions of oxide precursors over the full composition range.[5] The robot synthesized over 18 000 samples and successfully generated a range of new cuprate superconductors.[6,7] These authors were quite modest about the methodological revolution in which they were engaged, and a cursory description of their method appeared only in the experimental details of their papers. It was not highlighted in the abstracts. They reemphasized Hanak's view with the comment; "The usual method of superconductor synthesis involves repeatedly grinding and firing mixtures of oxide, carbonate and nitrate powders. This is tedious, expensive and can also be hazardous."[5] It can be argued retrospectively that their searches were constrained to cuprates, were slow compared with some current high-throughput methods, and lacked the computational capability for data mining that is now at hand, but the GEC contribution to combinatorial ceramic science is a landmark in its history.

There are two approaches to preparation of ceramic libraries: thick film and thin film. Thin film methods make use of vapor deposition or sputtering techniques by either masking or using multitarget chambers to produce submicrometer film and have been used, among others, in searches for superconductors,[8] for phosphors,[9] for dielectric properties using a noncontact probe,[10] and for fuel cell anode materials.[11]

Thick film methods make use of, inter alia, ink-jet printers and can employ the same commercially available powders that are used in manufacturing.[3,12,13] Ink-jet printers can produce ceramic samples of a few micrometers or several millimeters, for example, in the form of pillars, and can produce specific shapes, such as rings or lines or, indeed, other patterns. The minimum diameter depends on the surface properties of the substrate and liquid and can be as low as 100 μm.

Ink-jet printers have been used extensively in biotechnology[14−16] and polymer[17] research to make arrays of compositions. The use of direct ink-jet printing in ceramics is well-advanced, and 3-D ceramic architectures[18−20] including functionally graded structures[21] are produced. Not surprisingly, this technique has been applied to the preparation of combinatorial libraries using direct mixing of powder suspensions[12,13] and printing of ceramic precursor solutions.[22,23] Ink-jet printing has been successfully used for metal catalyst discovery and for precursors based on metal salts and alkoxides.[24]

Ink-jet printers can mix ink in three ways. In conventional color printers, separate colored droplets are placed adjacent to each other; color mixing actually occurs in the observer's

* To whom correspondence should be addressed. E-mail: j.r.g.evans@qmw.ac.uk.

10.1021/cc050006q CCC: $30.25
Published on Web 08/06/2005

Table 1. Specifications for the Aspirating−Dispensing Combinatorial Printer[a]

dispensing range	20 nL−250 μL
dispensing accuracy	±7% at 20 nL, ±5% at 100 nL
dispense to dispense precision[b]	<10% CV at 20 nL, <7% CV at 100 nL <5% CV at 1 μL
minimum aspiration volume	5 μL

[a] See ref 24. [b] CV, coefficient of variation.

brain. Applied to ceramic powders, this discrete printing approach involves large diffusion distances during sintering but has been used to print libraries from ceramic precursors in solution.[22] Mixing can also take place in the pipe-work behind the nozzles, a technique successfully used in ceramic combinatorial work and for preparing functional gradients.[12,21] Ceramic inks from multiple reservoirs pressurized with nitrogen are supplied via electromagnetic valves to a manifold. Variation in the opening times provides precise composition while a solenoid micropump provides circulation and mixing. After mixing, the ink is printed through an electromagnetic valve−nozzle assembly.[12,13] In this method, the number of ceramics that can be mixed is dependent on the number of reservoirs but the device can deposit large quantities and build functionally graded components.

The third approach, used in the London University Search Instrument (LUSI) robot, is to mix inks ahead of the nozzle by reformatting well plates. Stepper-driven syringes control aspiration and dispensing of ceramic suspensions. Miniature electromagnetic valves provide ink-jet printing. This approach, discussed in this paper, allows a very large number of components to be mixed while retaining the patterning capability of the printer.

Experimental Details

Description of the Instrument. The printer (ProSys 4510, Cartesian Ltd, Huntingdon, Cambridge) is based on SynQUAD dispensing technology in which electromagnetic valves are backed up by stepper-driven syringes (200 000 steps acting on 1.5 mL). This means that the valve can be opened to allow aspiration and dispensing as well as being pulsed to allow ink-jet printing from a line pressurized by the syringe. The specifications for dispensing and aspirating[25] are described in Table 1. Figure 1 shows the printer. The printer head is fitted with eight nozzles, each providing independent dispensing. The nozzles can automatically visit a cleaning station for purging, ultrasonic cleaning, and convective air-drying. The printer head can move with 1 μm nominal resolution in the $x-y-z$ directions on a 425 mm × 540 mm table holding one hundred 76 mm × 25 mm ceramic substrates. The printer is controlled by proprietary AxSys software that is used to program complex sequences of tasks involving well plate reformatting from compositional specifications read from a spreadsheet and ink-jet printing onto the library substrates.

The furnace was custom-built by Elite Thermal Systems Ltd, Leicestershire, UK. It has four chambers, individually heated and controlled. The maximum operating temperature is 1600 °C. The top half of the furnace can be raised into the vertical position to allow the robot to load and unload samples.

The measurement table measures 500 mm × 600 mm and is precise to 1 μm, subject to temperature fluctuation. A hot plate (Elmatic Ltd, Cardiff, UK) is mounted on the table and is independently controlled up to 250 °C and used to measure the temperature dependence of, for example, dielectric properties.

The printer, the furnace, and the measurement table are all contained within a robotic gantry manufactured by Labman Automation Limited, Stokesley, UK, and are shown in Figure 2. The robotic gripper can pick up each substrate from the printer table and move it from one stage to the next to a specified $x-y-z$ position with 100 μm resolution.

The data gathered from the instrument are stored in an Oracle database running on a dual 400 MHz, R12000 processor SGI Origin 3200 computer equipped with 1 GB of memory. Sample details are automatically recorded, including composition, the raw and processed results from measurements performed on it, and the assays of the inks used to create it. Figure 3 is a schematic of the operation.

Ceramic Ink Preparation. Water-based Al_2O_3, ZrO_2, and TiO_2 inks were prepared for calibration from readily available commercial powders. Table 2 describes the materials used in the inks, and Table 3 (rows 1−3) gives the compositions of the separate ZrO_2, TiO_2, and Al_2O_3 inks, respectively. For preparation of each ink, the constituents listed in Table 3 (rows 1−3) were mixed and subjected to dispersion using ultrasound under an ultrasonic probe (model U200S, IKA, Staufen, Germany) pulsed at 0.5 Hz and 75% amplitude for 1 ks.

In addition, a $BaTiO_3$ ink was prepared in the same way, but the mixture was left to sediment for 300 s and then decanted. The composition was found, post facto, from loss on ignition experiments. This ink contained 53.9 wt % $BaTiO_3$, 7.7 wt % dispersant, and 38.4 wt % distilled water.

Compositional Calibration. The process sequence for preparing ceramic compositions using this printer is illustrated in Figure 4. The printer transfers specified volumes of several ceramic inks from the source well plate into a well in the target plate to create a target composition. In this way, binary ink mixtures of powders A and B containing mass fraction m_A of powder A were made by aspirating a volume V_A ink to give a total volume V,

$$V_A = \frac{V}{\frac{\Phi_A \rho_A}{\Phi_B \rho_B}\left(\frac{1}{m_A} - 1\right) + 1} \tag{1}$$

where ρ_A and ρ_B are the densities, and Φ_A and Φ_B are the volume fractions of powder in the respective inks.

Drying at 60 °C to constant mass and loss on ignition at 700 °C in air were conducted to confirm composition and uniformity of composition so that the weight of dissolved powder could reliably be calculated from the volume of ink. The sedimentation behavior was studied by placing three 10 mL samples of Al_2O_3, ZrO_2, and TiO_2 ink in glass tubes. These were sealed, and the inks were left undisturbed to settle through the period of study. A further examination was made for sediments in the mixed well plate after mixing these inks; such sediments might result from interaction of particles.

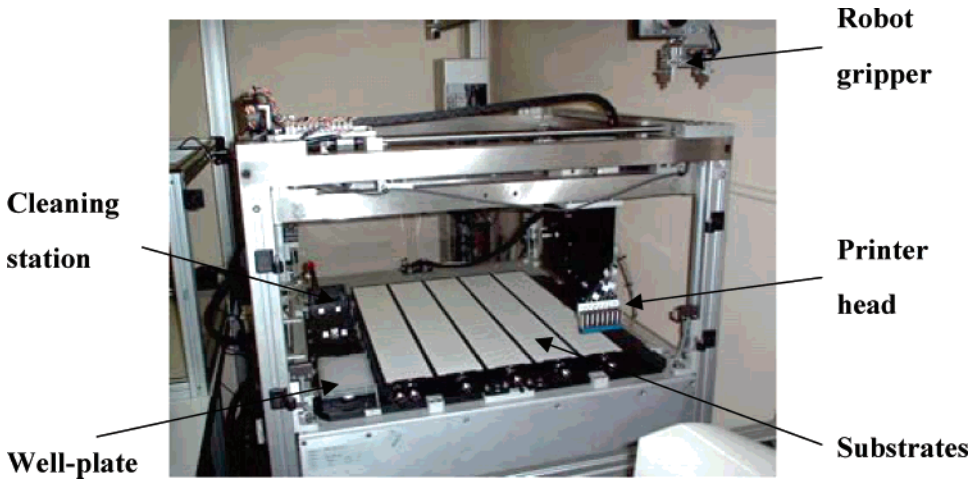

Figure 1. The ink-jet printer table within the robot gantry, populated with alumina substrates. The pick and place robot arm is seen in the top right.

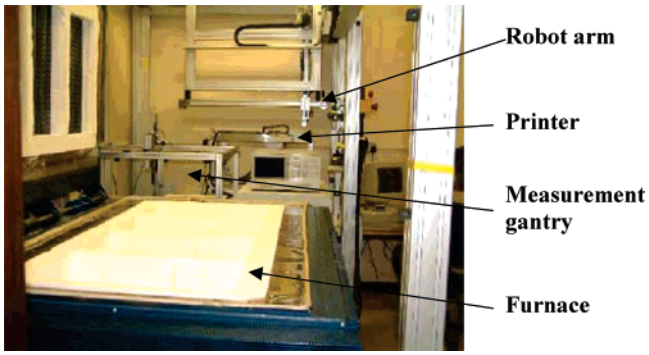

Figure 2. A view along the robot gantry from the furnace end showing the measurement table on the left.

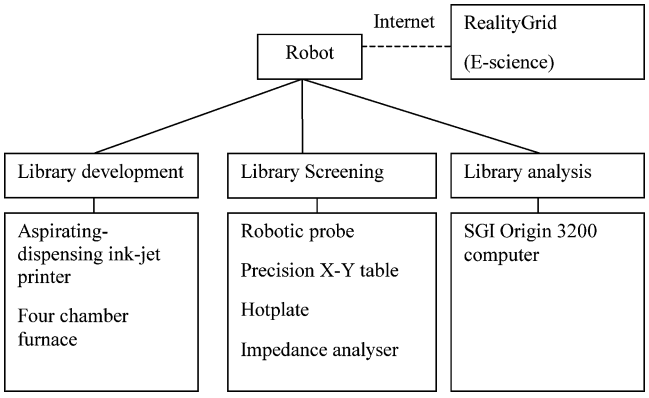

Figure 3. Schematic diagram of the combinatorial system.

Evaporation from the well plates was studied to assess how evaporative loss changes the weight percentage of ceramic in water-based inks in the well plate as a function of time. A well of the 96-well microplate was filled with ZrO_2 ink and then weighed on a four-place balance. A cover was put on the well plate after filling with ink. A 2 mm diameter perforation central to each well was made in the cover to allow the printer nozzles to penetrate it. Initially, commercially available silicone rubber well plate covers were used, but there was a risk of fracturing a ceramic nozzle on these, and so paper covers, usually of silicone release paper, were used. At a room temperature of 26 °C, the evaporative loss of inks from the well plate was recorded as a function of time.

The specification for the printer (Table 1) gives finite accuracy for printer transfer volumes, so the overall performance of the printer for well plate reformatting of ceramics was assessed by examining whether the printer can transfer a specified amount of powder dispersed as an ink to the target well plate. Four calibration compositions in the $Al_2O_3-TiO_2-ZrO_2$ system were transferred from source to target as though for mixing, but into separate crucibles.

A binary composition, 50 wt % ZrO_2 and 50 wt % TiO_2, and a ternary composition, 25 wt % Al_2O_3 and 25 wt % TiO_2 and 50 wt % ZrO_2, were printed and subjected to energy dispersive X-ray spectrometry (EDS) to assay the dried library mixtures after ink-jet deposition of printer-mixed composite inks. After reformatting the target well plate with new compositions, the printer aspirated the mixtures and dispensed 5 μL onto a porous cellulose nitrate membrane (Whatman International Ltd, Maidstone, UK). After air-drying for 1.8 ks they were removed from the cellulose nitrate membrane for EDS analysis without firing.

The printed samples were in the form of disks with a radius of ~1 mm. The top surfaces, the lower surfaces, and the cross sections were chemically analyzed for the distribution of cations. The samples were coated with carbon and studied by scanning electron microscopy (SEM; model 6300, JEOL, Tokyo, Japan) equipped with an EDS system (Oxford Instruments). Measurement was taken over an area approximately 150 μm × 150 μm for the surface and 50 μm × 50 μm for the cross section for a period of 100 s. These areas are sufficiently large to avoid the effect of powder agglomerates. The conditions for EDS analysis were 20 kV acceleration voltage and 15 mm working distance. The data were corrected using INCA software (Oxford Instruments). Cobalt was used as a standard for calibration of the analyzer.

Calibration of Dielectric Measurement on Combinatorial Samples. Figure 5 illustrates the procedure for dielectric measurement. With the well plate filled with $BaTiO_3$ ink and a platinum-coated 99.7% alumina slide positioned on the printing platform, the printer aspirated and dispensed 8.5 μL of $BaTiO_3$ drops onto the substrate. After printing, the robot transferred the substrate from the printer platform to the furnace, where the sample was fired at 1400

Table 2. Materials and Sources Used for Water-Based Ceramic Inks

material	supplier	grade	purity %	density/kgm^{-3}	av particle size/μm
Al_2O_3	Alcoa; Ludwigshafen, Germany	A16-SG	99.8	3987	0.5
TiO_2 (Anatase)	Tioxide Europe SA; Calais, France	A-HR	99.0	3850	0.15
ZrO_2	Pi-Kem; Shropshire, UK		99.5	5750	0.9
$BaTiO_3$	TPL Inc, NE; Albuquerque, NM	HPB 1000		5700	0.05
dispersant	Allied Colloids Ltd; Bradford, UK	Dispex A40		1300	

Table 3. Table of Ceramic Ink Compositions

planned composition	Al_2O_3 powder wt %	TiO_2 powder wt %	ZrO_2 powder wt %	dispersant wt %	distilled water wt %
100 wt % ZrO_2			38.83	1.52	59.65
100 wt % TiO_2		29.93			70.07
100 wt % Al_2O_3	30.46			0.77	68.77
25 wt %Al_2O_3 25 wt %TiO_2 50 wt % ZrO_2	8.49	8.49	16.98	0.88	65.16
25 wt %Al_2O_3 25 wt %TiO_2 50 wt % ZrO_2	8.49	8.49	16.98	10	56.04

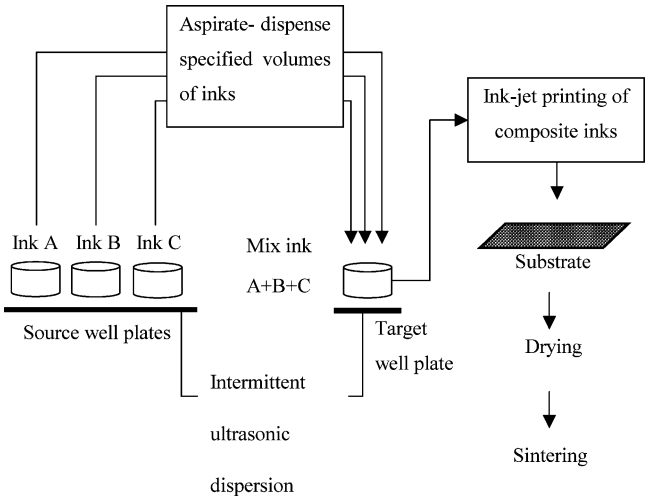

Figure 4. Schematic diagram of the mixing and printing protocol.

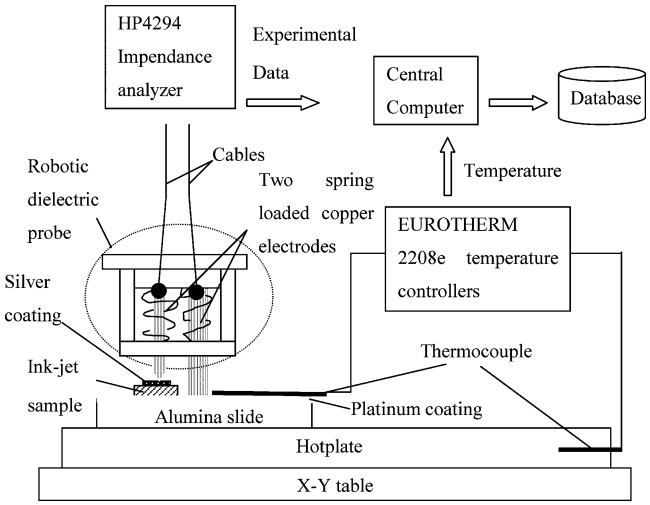

Figure 5. The experimental arrangement for combinatorial dielectric measurement.

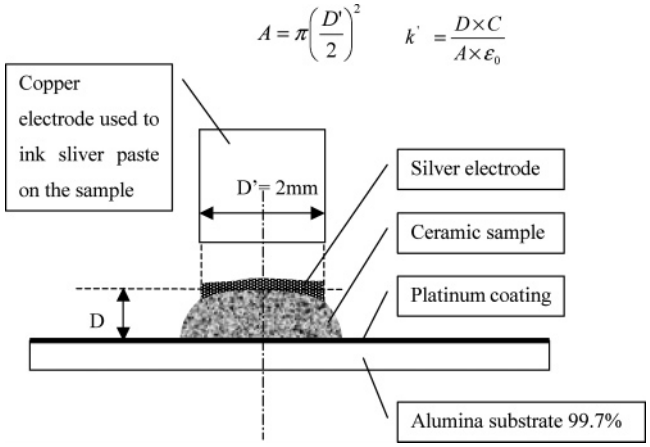

Figure 6. The geometry of fired ink-jet-printed ceramic on the platinum-coated substrates.

°C for 7.2 ks in air. The robot repositioned the substrate onto the $x-y$ table, where the probe deposited silver paste on the sample by a stamping operation. The robot then took the substrate back to the furnace, where the electroded samples were fired at 800 °C for 300 s. The robot then replaced the substrate on the $x-y$ table, and the spring-loaded dielectric probe, activated by the robot arm, made contact with the sample and the adjacent ground electrode. The frequency dependence of capacitance from 100 Hz to 1 MHz at room temperature was measured by the HP4294 impedance analyzer. The temperature dependence of capacitance was measured by tracking the capacitance from 180 °C as the hot plate slowly cooled (maxiumum cooling rate was controlled at 3.4 °C/min) at 1 kHz using a foil thermocouple adjacent to the sample. The impedance analyzer transferred data to the central control computer where the measurement data were available to be processed as required. The data were converted to database structure and stored in the database.

Figure 6 describes how the values of thickness, *D*, and area of the electrode of the capacitor, *A*, were determined. The sample diameter was kept above 2 mm to allow the electroded region to approximate to a parallel plate configuration, although smaller and, hence, more curved-top electrodes can be used with a geometrical correction. The thickness of fired samples, *D*, was measured by micrometer.

Table 4. Results of Loss on Ignition of Transferred Inks[a]

planned transfers/g			mean actual transfers/g (CV%)[b]			
ZrO_2	Al_2O_3	TiO_2	ZrO_2	Al_2O_3	TiO_2	error mass %[c]
0.105	0.105		0.106	0.106		0.07
	0.088	0.088		0.087	0.088	0.3
0.104		0.104	0.104		0.103	0.2
0.105	0.052	0.052	0.104	0.052	0.053	0.1/0.2/0.3

[a] Each result is the mean of three trials. [b] Coefficient of variation. [c] This is the error in the mass % of each oxide in the delivered mixture as calculated before truncating the transfers to 3 significant figures.

The dielectric results were compared with literature values and with the results from ceramic samples that were produced in conventional ways. Pellets of $BaTiO_3$ powder were pressed at 35 MPa and sintered at 1400 °C for 7.2 ks in air and then abraded to give flat parallel sides. These were metallized using silver paste to form a parallel plate capacitor. Both temperature dependence (from 180 °C to room temperature at 1 kHz) and frequency dependence (from 100 Hz to 1 MHz at room temperature) of capacitance were measured by the impedance analyzer. To explore how the measurement was affected by geometry, the printer dispensed 150 μL of $BaTiO_3$ ink into a shallow mold. The resulting sample was dried for 3.6 ks, fired at 1400 °C for 7.6 ks in air, and abraded to give flat, parallel sides. The two faces were painted with silver paste, the sample was fired at 800 °C for 5 min, and the sides were abraded to give a rectangle. The dielectric properties were measured and compared with the pressed sample.

Results and Discussion

Ink Assays. The sedimentation results showed Al_2O_3, ZrO_2, and TiO_2 ink were stable for at least 7.2 ks after preparation, and these inks were used in experiments for compositional calibration of the printer. Because no printer programs run for more than 7.2 ks and the well plate holding these inks is subject to intermittent ultrasonic dispersion, these inks have adequate stability during the running of a printing program. To control evaporation of inks, the well plate should be refilled with fresh ink at every 1.8 ks (i.e., 30 min) during the operation to keep the error in weight percentage of ceramic within 1 wt %.

Table 4 gives loss on ignition of transferred inks for four compositions in the $Al_2O_3-TiO_2-ZrO_2$ system and, hence, compares the individual masses transferred with those programmed. The total volume of these calibration inks was 0.45 mL. The errors associated with the transferred masses in Table 4 are calculated in two ways. The coefficient of variation from the three trials for each composition is given in brackets as a percentage and defines the variation associated with an individual transfer of one component of the mixture. These vary between 0.3 and 1.4%. The final column gives the compositional error in weight percent for that mixture based upon the means. The maximum error was 0.3 wt %. These errors can be attributed in part to the inaccuracy of printer dispensing. From Table 1, there is a manufacturer's quoted error of ±5 vol % at 100 nL, which was the base dispensing unit in all printer programs. In fact, the error is considerably less than this. Evaporative loss also contributes. Finally, there is an error associated with the gravimetric measurement.

Table 5. Average EDS Analysis for Calibration Samples Mixed and Printed by the Aspirating−Dispensing Printer onto a Porous Substrate

	EDS analysis/wt %[a]		
planned composition/wt %	top surface	lower surface	cross section
TiO_2, 50	50	53	49
ZrO_2, 50	50	47	51
Al_2O_3, 25	25	27	26
TiO_2, 25	24	26	25
ZrO_2, 50	51	47	49

[a] Average for three arrays at different positions.

These oxides were selected because the X-ray Kα energies of the metals are well-separated and, therefore, easily distinguished by EDS. Table 5 gives average EDS analysis results for calibration samples mixed and printed by the aspirating−dispensing printer by depositing on a microporous cellulose nitrate membrane, which allows rapid drying by capillary flow into the substrate. These compare with the programmed composition to within 1−3 wt % (Table 5), which is the error that is to be expected from EDS analysis of unpolished surfaces.[26]

Geometry and Compositional Distribution of Dried Ink-Jet-Printed Samples. It was found that changing the amount of dispersant used in the ceramic inks can be used to achieve better sample geometry for property measurements and a uniform planned composition of droplet residues. Taking the ternary composition, 25 wt % Al_2O_3, 25 wt % TiO_2, and 50 wt % ZrO_2, as an example, the ink compositions of Table 3 (rows 4 and 5) were manually weighed, mixed, and subjected to ultrasonic dispersion at 0.5 Hz and 75% amplitude for 1 ks. Droplets of the mixtures were deposited onto silicone release paper from a fine wire and left in air for 3.6 ks. After drying, they were photographed and then lifted from the silicone release paper and subjected to EDS analysis.

For the ink containing a small amount of dispersant (Table 3, row 4), the residues from the ink droplets had "doughnut" shapes, sometimes with a hole in the middle (Figure 7a). Segregation of powders was found on the upper surface of residues (Table 6, row 1). Similar droplet residue profiles are obtained from ink-jet-printed ceramic libraries prepared from precursor solutions.[23] A flatter upper surface is required for contact dielectric measurements.

Ink containing a large amount of dispersant (Table 3, row 5), much more than that needed to inhibit sedimentation, had uniform planned composition and presented a dome shape, as shown in Table 6, row 2, and Figure 7b, respectively. The EDS method is capable of an accuracy of 2 wt %. Both the shape and the segregation are related to migration of liquid and particles during droplet drying.[27] Both effects are seen in drops deposited by the printer and in samples gravimetrically mixed and manually deposited. The volume fraction of powder in the dried residue from these droplets was ~0.76 so that the assembly of particles could sinter to full density once the organic constituents was removed by

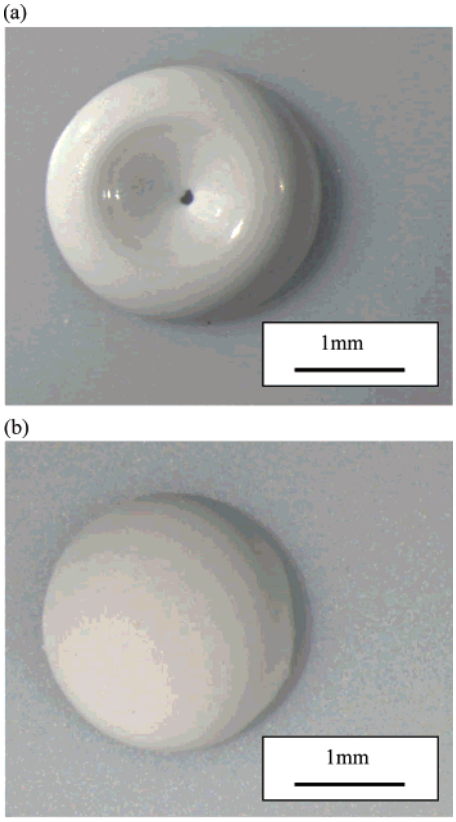

Figure 7. The shapes of residues of droplets of ceramic inks deposited on silicone release paper: (a) ceramic inks with 0.88 wt % dispersant and (b) ceramic inks with 10 wt % dispersant.

Table 6. Effect of Excess Dispersant on Compositional Uniformity of Dried Ceramic Ink[a]

		EDS analysis/wt %		
ink designation	planned composition wt %	top surface	lower surface	cross section
Table 3, row 4 (containing 0.88 wt % dispersant)	Al_2O_3, 25	12 ± 11	26 ± 1	25 ± 2
	TiO_2, 25	9 ± 12	24 ± 0	24 ± 2
	ZrO_2, 50	79 ± 22	50 ± 1	51 ± 3
Table 3 row 5 (containing 10 wt % dispersant)	Al_2O_3, 25	25 ± 1	26 ± 0	24 ± 1
	TiO_2, 25	25 ± 1	23 ± 0	24 ± 1
	ZrO_2, 50	50 ± 1	51 ± 0	52 ± 1

[a] Average for five arrays with 95% confidence interval.

pyrolysis. This is one method to ensure a uniform planned composition throughout. The other, illustrated here in the results in Table 5, is to print onto a porous substrate, such as microporous cellulose nitrate paper, so that droplet drying and, hence, the formation of a rigid particle network is rapid.

Dielectric Measurements. ASTM designation D150-87 (1989, section 10) specifies the conditions for measuring the dielectric constant and dissipation factor. For high accuracy, the guarded electrode method is preferred, but for routine work, the unshielded two-electrode system is accepted and is used here. In combinatorial work, there is necessarily a tradeoff between accuracy and miniaturization for high throughput. The greatest error is regarded as lying in the measurement of dimensions. The "unequal electrodes"

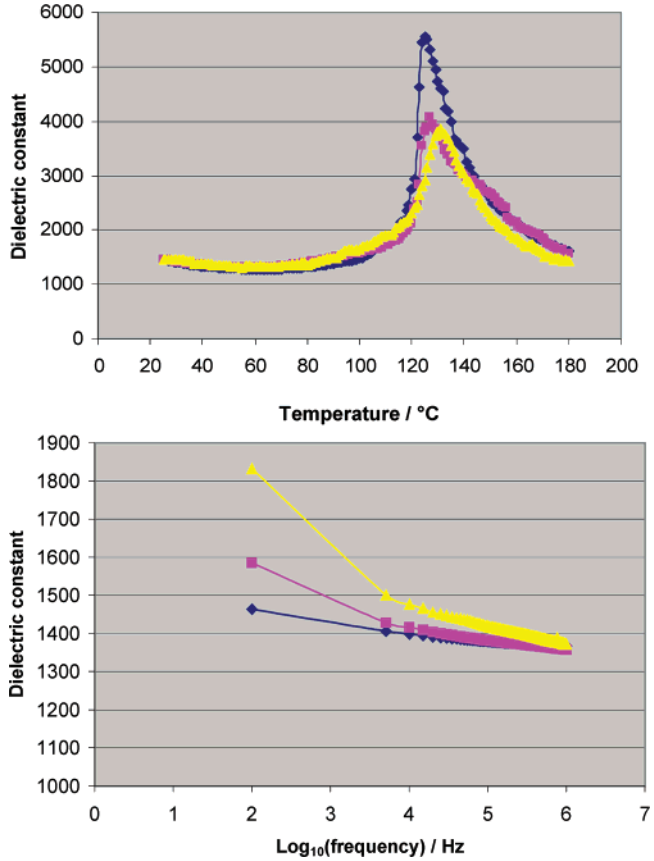

Figure 8. Temperature and frequency dependencies of dielectric constants of $BaTiO_3$. ◆, Pressed $BaTiO_3$; ■, $BaTiO_3$ ink dried in a mold; ▲, ink-jet-printed $BaTiO_3$ on platinum-coated substrates measured by the dielectric probe in the combinatorial robot.

method given in Table 1 of the ASTM designation was used. The corresponding empirical stray field correction, which depends mainly on the electrode perimeter, *P*, gives errors in the region of 3−3.5%. This correction becomes more significant as the sample size decreases and is therefore relevant for combinatorial procedures.

As a supplementary check on the measurement method, a series of metallized polypropylene radial capacitors with 1% tolerance (RS Components, Derby, UK) were tested using the same baseline before making sample measurements and gave values within the tolerance range.

A displacement transducer can be fitted to the probe station to record the sample and ground electrode levels, but in the present work, thickness was measured with a micrometer. The thicknesses of the three types of sample, (i) compacted $BaTiO_3$, (ii) samples prepared from ink and dried in a mold, and (iii) ink-jet-printed samples on platinum-coated 99.7% alumina substrates, were 2.13, 0.8, and 0.36 mm, respectively. This experiment distinguishes the effect of the preparation method (compaction compared with ink deposition) from geometrical effects (disks compared with droplet relics). Figure 8 shows the measured temperature and frequency dependence of dielectric constants of $BaTiO_3$.

The results for samples prepared by drying $BaTiO_3$ ink and ink-jet-printed $BaTiO_3$ on platinum-coated substrates measured automatically by the dielectric probe agree with those for the conventional compacted sample in the lower range of dielectric constant. As shown in Figure 5, the foil

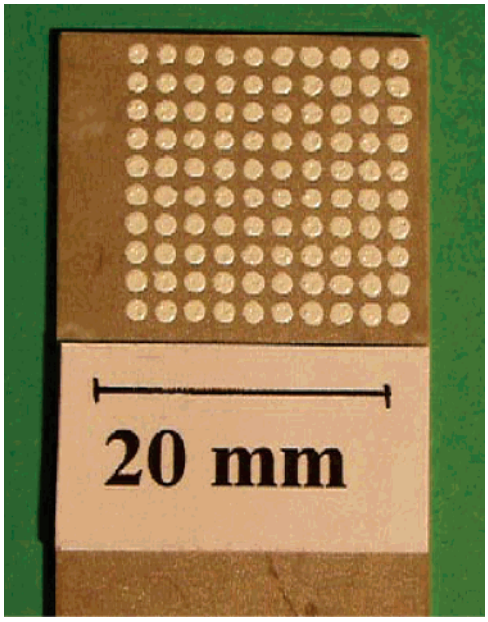

Figure 9. An array of samples printed to give a library density of 2.5×10^5 m^{-2}.

thermocouple was placed adjacent to the sample and the recorded temperature can deviate slightly from the sample temperature as seen in Figure 8 for the Curie temperature. For the conventional sample, the thermocouple was central and in direct contact. The peak permittivity is sensitive to the preparation method and was lower for samples prepared from ink, whether dried in bulk or ink-jet-printed, compared with the pressed disk. The peak value for the pressed disk, in turn, is lower than the literature values, which give peaks in the region of 9500.[28,29] The main cause is fired density. The relative density of the pressed disk was 94%, and the samples prepared from ink appear to have a lower density, as deduced from scanning electron microscopy. Thus, higher firing temperature may be needed to establish the same density from material prepared in the form of an ink in a combinatorial routine to samples prepared by conventional compaction with consequences for grain size, which is known to influence dielectric properties.[30] Figure 8 also shows that the frequency dependence of the dielectric constant is consistent between samples.

Figure 9 shows 100 samples, each 0.2 μL, printed on a 20 mm square, giving a library density of 2.5×10^5 m^{-2} in a cubic array. It has additional space for placing a second probe adjacent to each sample to avoid the inductive effect of a long and variable conduction path to a common electrode on each tile. The platinum coating was prepared by evaporation on alumina substrates.

Automation in a Distributed System. The time (in seconds) used in the combinatorial method is

$$t = [t_P(N, S) + t_F(X \times 54, Y) + t_M(X \times 45 + S \times 20 + 86.4 \times 10^3) + t_S + t_A + 360] \times n \quad (2)$$

where, t_P is the time for the printer to reformat the well plate and print samples on the substrate. This is a function of the number of compositions created, N, and the number of printed samples, S; n is the number of cycles. One composition may be printed as several copies to allow firing at different temperatures to explore processing as well as compositional parameters or to provide an assessment of error by replication. This base time depends on the number of components in the system and the sequence chosen for mixing and printing. It can be reduced by, for example, printing in flight, and the printer has this ability. t_F is a function of the number of printed library substrates, X, and the firing program, Y. The robot takes ~54 s to transfer one substrate from the printer to the furnace and return to its home position. The firing program, Y, varies as the experiment requires and provides the greatest time penalty. t_M is the time required for printing metallized electrodes; it takes ~45 s for the robot to replace a substrate from the furnace to the hot plate and vice versa. It takes ~30 s to deposit silver paste on the top of each sample and 86.4 ks for the furnace to fire the metallized samples to 800 °C for 300 s and to cool naturally to 50 °C. t_S and t_A are the times spent screening the library and analyzing the library, respectively, which are both experiment-dependent. During one cycle, the furnace door closes and opens twice, which costs 360 s. The time required for ink preparation is excluded; it is assumed that inks are available from stock. On this basis, the times given are not sensitive to the oxide types.

The whole system can perform unlimited operations with minimum human intervention. LUSI is a unique instrument, and therefore, it is desirable to make it available through e-science networks. The evolving paradigm for sharing computational and experimental resources over the Internet is the Grid. RealityGrid[31] is a leading UK e-science project that has as one of its aims the integration of LUSI into the Grid. Thus, alongside molecular modeling and the associated visualization methods which are presently being grid-enabled, we may begin to envisage combinatorial laboratories in which geographically diffuse operators steer searches on the basis of their own computer-assisted analysis of the emerging data.

Clearly, a range of machine learning algorithms, such as those provided by artificial neural networks (weak methods) to those capable of specifying the nature of connections (strong methods), are becoming available. Thus, when informatics is combined with combinatorial methods, it then becomes necessary to distinguish the terms "high-throughput screening" from "combinatorial" methods. The former implies a screen or mesh through which unwanted (not optimized) compositions pass to waste while the latter implies that all data are collected, stored, and assessed for the creation of wider and more general knowledge. These important issues are discussed in greater depth in current texts.[32−34] A controversy surrounds the application of informatics to scientific discovery: it is claimed by some that hypothesis-free experiments, from which "in silico" or machine learning can generate new theory, can never be conducted.[35] One can discern the fallacy of converse accident in this criticism. It is rarely the intention, and may not be a possibility, to conduct hypothesis-free experiments. The choice of starting materials and even the measurement methods are "theory-laden", and the perceived uses of these methods should be seen, and are being used as, a way of speeding up what is

often already an empirical approach to scientific discovery in areas for which predictive theory is inadequate, rather than the complete exclusion of human intervention.

Conclusions

An aspirating and dispensing combinatorial printer established inside a robot gantry equipped with a furnace and measurement table is described. It can assemble ceramic mixtures with compositional accuracy of 1−3 wt % when precautions are taken to establish stability against sedimentation, evaporation of vehicle, and particle segregation on drying. The same material prepared in three ways, in the form of dried ink, ink-jet-printed as for a combinatorial sample, and by conventional compaction, gave similar dielectric measurements. By changing the amount of dispersant used in the inks or by printing onto a porous substrate, the geometry of residues from dried ceramic ink droplets can be modified to facilitate property measurements, and uniform composition, as planned, can be achieved. In this way, the London University Search Instrument has been established as a combinatorial system so that combinatorial libraries can be printed, fired, and screened automatically.

Acknowledgment. The authors are grateful to the Engineering and Physical Sciences Research Council for funding this instrument under Grant No. GR/R06977.

References and Notes

(1) Yang, S.; Evans, J. R. G. *J. Comb. Chem*. **2004**, *6*, 549−555.
(2) Meier, M. A. R.; Hoogenboom, R.; Schubert, U. S. *Macromol. Rapid Commun.* **2004**, *25*, 21−33.
(3) Evans, J. R. G.; Edirisinghe, M. J.; Coveney, P. V.; Eames, J. *J. Eur. Ceram. Soc*. **2001**, *21*, 2291−2299.
(4) Hanak, J. J. *J. Mater. Sci.* **1970**, *5*, 964−971.
(5) Hall, S. R.; Harrison, M. R. *Chem. Brit.* **1994**, *30*, 739−742.
(6) Beales, T. P.; Freeman, W. G.; Hall, S. R.; Harrison, M. R.; Parberry, J. M. *Physica C* **1993**, *205*, 383−396.
(7) Beales, T. P.; Dineen, C.; Freeman, W. G.; Hall, S. R.; Harrison, M. R.; Jacobson, D. M.; Zammattio, S. J. *Supercond. Sci. Technol*. **1992**, *5*, 47−49.
(8) Xiang, X. D.; Sun, X. D.; Briceno, G.; Lou, Y. L.; Wang, K. A.; Chang, H. Y.; Wallace-Freedman, W. G.; Chen, S. W.; Schultz, P. G. *Science* **1995**, *268*, 1738−1740.
(9) Wang, J. S.; Yoo, Y.; Gao, C.; Takeuchi, I.; Sun, X. D.; Chang, H. Y.; Xiang, X. D.; Schultz, P. G. *Science* **1998**, *279*, 1712−1714.
(10) Chang, H.; Gao, C.; Takeuchi, I.; Yoo, Y.; Wang, J.; Schultz, P. G.; Xiang, X. D.; Sharma, R. P.; Downes, M.; Venkatesan, T. *Appl. Phys. Lett*. **1998**, *72*, 2185−2187.
(11) Strasser, P.; Fan, Q.; Devenney, M.; Weinberg, W. H.; Liu, P.; Norskov, J. K. *J. Phys. Chem. B* **2003**, *107*, 11013−11021.
(12) Mohebi, M. M.; Evans, J. R. G. *J. Comb. Chem*. **2002**, *4*, 267−274.
(13) Mohebi, M. M.; Evans, J. R. G. *J. Am. Ceram. Soc*. **2003**, *86*, 1654−1661.
(14) Lemmo, A. V.; Rose, D. J.; Tisone, T. C. *Curr. Opin. Biotechnol.* **1998**, *9*, 615−617.
(15) Lemmo, A. V.; Fisher, J. T.; Geysen, H. M.; Rose, D. J. *Anal. Chem.* **1997**, *69*, 543−551.
(16) Cargill, J. F.; Lebl, M. *Curr. Opin. Chem. Biol.* **1997**, *1*, 67−71.
(17) de Gans, B. J.; Schubert, U. S. *Macromol. Rapid Commun*. **2003**, *24*, 659−666.
(18) Bhatti, A. R.; Mott, M.; Evans, J. R. G.; Edirisinghe, M. J. *J. Mater. Sci. Lett*. **2001**, *20*, 1245−1248.
(19) Zhao, X.; Evans, J. R. G.; Edirisinghe, M. J.; Song, J. H. *J. Mater. Sci*. **2002**, *37*, 1987−1992.
(20) Zhao, X. L.; Evans, J. R. G.; Edirisinghe, M. J.; Song, J. H. *J. Am. Ceram. Soc*. **2002**, *85*, 2113−2115.
(21) Mott, M.; Evans, J. R. G. *Mater. Sci. Eng., A* **1999**, *271*, 344−352.
(22) Okamura, S.; Takeuchi, R.; Shiosaki, T. *Jpn. J. Appl. Phys*. **2002**, *41*, 6714−6717.
(23) Sun, X. D.; Wang, K. A.; Yoo, Y.; Wallace Freedman, W. G.; Gao, C.; Xiang, X. D.; Schultz, P. G. *Adv. Mater*. **1997**, *9*, 1046.
(24) Schneemeyer, L. F.; van Dover, R. B. High Throughput Synthetic Approaches for the Investigation of Inorganic Phase Space. In *Experimental Design for Combinatorial and High Throughput Materials Development*; Cawse, J. N., Ed.; John Wiley & Sons, Inc.: New York, 2003; pp 55−71.
(25) System Operating Manual, version 1.0; Prosys Gantry System; Cartesian Technologies: Huntingdon, Cambridge, June 2000.
(26) Scott, V. D.; Love, G.; Reed, S. J. B. *Quantitative Electron-Probe Microanalysis*; Ellis Horwood: London, 1995; p 93.
(27) Wang, J.; Evans, J. R. G.; to be published.
(28) Moulson, A. J.; Herbert, J. M. *Electroceramics: Materials, Properties, Applications*; Chapman & Hall Press: London, 1997; p 249.
(29) Mitsui, T.; Abe, R.; Furuhata, Y.; Gesi, K.; Ikeda, T.; Kawabe, K.; Makita, Y.; Marutake, M.; Nakamura, E.; Nomura, S.; Sawaguchi, E.; Shiozaki, Y.; Tatsuzaki, I.; Toyoda, K. Numerical data and functional relationships in science and technology; Group III, Alle. Zeit. Wach Press, Springer-Verlag: Berlin−Heidelberg, New York, 1969; Vol. 3; pp 51, 247.
(30) Wang, X. H.; Chen, R. Z.; Gui, Z. L.; Li, L. T. *Mater. Sci. Eng., B* **2003**, *99*, 199−202.
(31) Coveney, P. V. http://www.realitygrid.org/news.html.
(32) Farrusseng, D.; Mirodatos, C. Combinatorial Strategies for Speeding up Discovery and Optimization of Heterogeneous Catalysts on the Academic Laboratory Scale: A Case Study of Hydrogeneous Purification for Feeding PEM Fuel Cells. In *High-Throughput Screening in Chemical Catalysis: Technologies, Strategies and Applications*; Hagemeyer, A., Strasser, P., Volpe, A. F., Jr., Eds.; Wiley-VCH: New York, 2004; pp 239−270.
(33) Holena, M.; Baerns, M. Artificial Neural Networks in Catalyst Development. In *Experimental Design for Combinatorial and High Throughput Materials Development*; Cawse, J. N., Ed.; John Wiley & Sons, Inc.: New York, 2003; pp 163−202.
(34) Breneman, C. M.; Bennett, K. P.; Embrechts, M.; Sukumar, N.; Cramer, S.; Song, M.; Bi, J. Descriptor generation, selection and model building in quantitative structure−property analysis. In *Experimental Design for Combinatorial and High Throughput Materials Development*; Cawse, J. N., Ed.; John Wiley & Sons, Inc.: New York, 2003; pp 203−238.
(35) Allen, J. F. *Bioessays* **2001**, *23*, 104−107.

CC050006Q